

# Optically Cooling CsPbBr<sub>3</sub> Nanoparticles

Authors: Benjamin J. Roman,<sup>1</sup> Matthew T. Sheldon\*<sup>1,2</sup>

## Affiliations:

<sup>1</sup>Department of Chemistry, Texas A&M University, College Station, TX, USA.

<sup>2</sup>Department of Materials Science & Engineering, Texas A&M University, College Station, TX, USA.

\*Correspondence to: sheldonm@tamu.edu

## Abstract:

One photon up-conversion photoluminescence is an optical phenomenon whereby the thermal energy of a fluorescent material is used to increase the energy of an emitted photon compared with the energy of the photon that was absorbed. When this occurs with near unity efficiency, the emitting material undergoes a net decrease in temperature—so called optical cooling. Because the up-conversion is thermally activated, the yield of up-converted photoluminescence is also a reporter of the temperature of the emitter. Taking advantage of this optical signature, here we show that cesium lead trihalide nanocrystals are cooled by as much as 66 K during the up-conversion of 532 nm CW laser excitation. This is the first demonstration of optical cooling of colloidal semiconductor nanocrystals, as well as a new record for optical cooling of any semiconductor system, highlighting the intrinsic advantages of colloidal nanocrystals for this goal.

## Main Text:

A remarkable property of semiconductors is their ability to produce photoluminescence via a mechanism of one photon up-conversion, also known as anti-Stokes photoluminescence (ASPL).<sup>1-3</sup> During ASPL, a photoexcited carrier is additionally excited by phonons in the semiconductor before radiatively relaxing. The result is the emission of a photon with energy greater than the photon that was absorbed. Further, the process scavenges thermal energy from the semiconductor, equivalent to the difference in energy between the incoming and outgoing photon. Intuitively, ASPL is thermally activated since it requires a population of phonons with appropriate energy to drive the up-conversion of the photoexcited carriers. Thus, the ASPL yield for a given sample is exponentially dependent on the energy difference between the pump wavelength and the emitted wavelength, as well as the inverse temperature of the material, following an Arrhenius relationship.<sup>2,4-6</sup> If this process occurs with an external quantum efficiency (EQE) near unity, more thermal energy is removed *via* ASPL than is added by thermalization due to nonradiative recombination, and the system will experience a net decrease in temperature.<sup>1</sup> This optically driven cooling has been a target of interest since it was first proposed as a vibrationless, solid state method of refrigeration for which optical excitation provides a remote power source.<sup>7</sup> More generally, ASPL has been explored as a mechanism to enable a variety of thermodynamic power cycles that can scavenge waste thermal energy.<sup>8,9</sup>

Theoretically, optically cooled semiconductors are predicted to be able to reach temperatures below 10 K;<sup>1,10</sup> despite this, optical cooling of bulk semiconductors has yet to be demonstrated. For net cooling to occur, the thermal energy scavenged by emitted photons—a few tens to a few hundreds of meV worth of energy for each emitted photon—has to be greater than the thermal

energy generated by non-radiative losses, with each non-radiative recombination contributing a full band gap worth of heat. As such, external quantum efficiencies must be greater than ~96% for optical cooling to occur. Despite having internal quantum efficiencies (IQE) exceeding 99%, high quality bulk semiconductors still have to contend with insufficient photon extraction efficiencies (i.e. too low EQE) due to total internal reflection and parasitic absorption from their surface passivation. These losses are largely an intrinsic feature of the macroscopic semiconductor geometry.<sup>11–13</sup>

In recent years, the first instances of measurable laser cooling of semiconductors have been reported by Xiong and coworkers. In their experiments, chemical vapor deposition was used to fabricate semiconductor morphologies that are subwavelength in size in at least one dimension, in order to maximize the optical extraction efficiency of the ASPL, i.e. to promote high EQE via better light management.<sup>14,15</sup> Until this study, their reports remained the only demonstrations of net optical cooling of a semiconductor, largely due to the difficulty of fabricating materials with sufficiently high quantum efficiencies. Alternatively, high quality colloidal semiconducting nanocrystals appear to ubiquitously show ASPL<sup>4</sup> and can be synthesized in subwavelength sizes with EQE's above the threshold required for net cooling.<sup>16</sup> Notably, recent works have identified all-inorganic cesium lead trihalide perovskite nanocrystals as a material with potential applications for optical cooling due to their near-unity photoluminescence quantum yield after appropriate surface treatment.<sup>2,3,17</sup> Additionally, recent works by our group and others have suggested that ASPL in CsPbX<sub>3</sub> (X = I, Br, or Cl) nanocrystals may not utilize mid-gap electronic trap states, as has been reported for other semiconductors.<sup>2,6,18</sup> The lack of mid-gap electronic states in CsPbX<sub>3</sub> is a desirable characteristic since it further reduces the chances of deleterious non-radiative recombination.

Here, we report for the first time the optically driven cooling of colloiddally prepared semiconducting nanocrystals—specifically CsPbBr<sub>3</sub> nanoparticles. We use the temperature dependence of the ASPL yield as a reporter for the temperature the nanocrystals obtain during below gap excitation. We show that the nanoparticles cool at an exponential rate before reaching a final saturation temperature, indicating the balance between the cooling power and heating from the environment. The rate of cooling, as well as the final temperature reached, are shown to be dependent on the excitation laser fluence. The lowest temperature recorded in this study is 232 K. At a net temperature decrease of 66 K, this represents a new record for the optical cooling of a semiconductor.

CsPbBr<sub>3</sub> nanoparticles were synthesized following the hot-injection method established by Protesescu and coworkers.<sup>19</sup> As prepared, CsPbBr<sub>3</sub> have EQE as high as 80%. Their EQE can be further increased to approximately unity with a treatment of NH<sub>4</sub>SCN. In this reaction, SCN<sup>-</sup> removes the excess lead atoms on the nanocrystal surface that are understood to be the predominant source of mid-gap states.<sup>20,21</sup> This is necessary because optical cooling requires that the nanocrystals have an EQE that overwhelms thermalization losses during absorption. The necessary EQE threshold for cooling can be calculated by considering the amount of thermal energy emitted with each photon, as defined by the anti-Stokes shift between the excitation wavelength and the emission wavelength.<sup>1</sup> In our study, 532 nm excitation of CsPbBr<sub>3</sub> produces PL centered around 517 nm (Figure 1), corresponding to an average anti-Stokes shift of approximately 70 meV. Our work and others' have established this as a one photon up-conversion process whereby absorption of multiple phonons converts below-bandgap absorption into band edge emission.<sup>2,3,5</sup> Thus, for every photon emitted, ~70 meV of thermal energy is

removed from the semiconductor. In contrast, every instance of non-radiative recombination adds 2.41 eV of thermal energy into this system. For the thermal energy emitted to be greater than the thermal energy added through non-radiative recombination, radiative recombination and emission into free space must occur with greater than 97.1% efficiency.

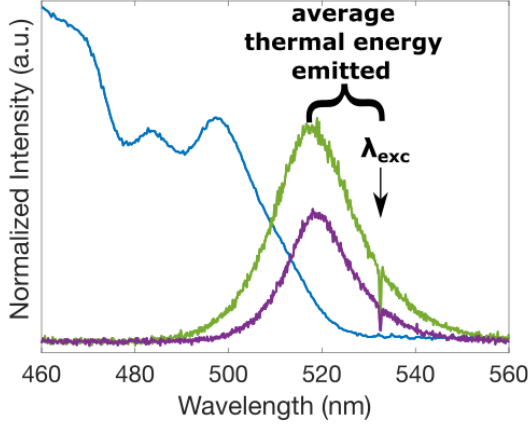


**Figure 1.** CsPbBr<sub>3</sub> anti-Stokes photoluminescence at 298 K (purple) and 338 K (green) plotted against CsPbBr<sub>3</sub> absorbance (blue).

In order to determine the change in the nanoparticle temperature during below gap excitation, it was necessary to develop a thermometry technique that was non-perturbative during the cooling of the nanoparticles. Previous reports have used the temperature dependence of the conventional Stokes shifted photoluminescence (SSPL) to determine the nanoparticle temperature.<sup>14,15</sup> This probe simultaneously heats the sample due to thermalization of the photoexcited carriers. As such, this technique cannot be used to actively monitor the nanoparticle temperature during cooling. Alternatively, ASPL is a thermally activated mechanism, so the amount of up-conversion at a fixed excitation wavelength and fluence is sensitive to the temperature of the emitting nanoparticles. As the nanoparticles are heated, the intensity of the ASPL increases, and conversely the ASPL decreases as the temperature of the nanoparticles decrease. We have previously shown that the temperature dependence of the ASPL intensity from CsPbBr<sub>3</sub> nanocrystals follows an Arrhenius relation, with the natural log of the intensity directly proportional to  $1/T$ .<sup>2</sup> Equation 1, thus, can be used to determine any given change in temperature based on the change in ASPL intensity, so long as one temperature is known.

$$T = T_0 * \frac{\ln(I)}{\ln(I_0)} \quad (1)$$

In this,  $I_0$  is the integrated ASPL intensity at some known temperature,  $T_0$ , and  $I$  is the integrated ASPL intensity at some new temperature,  $T$ .

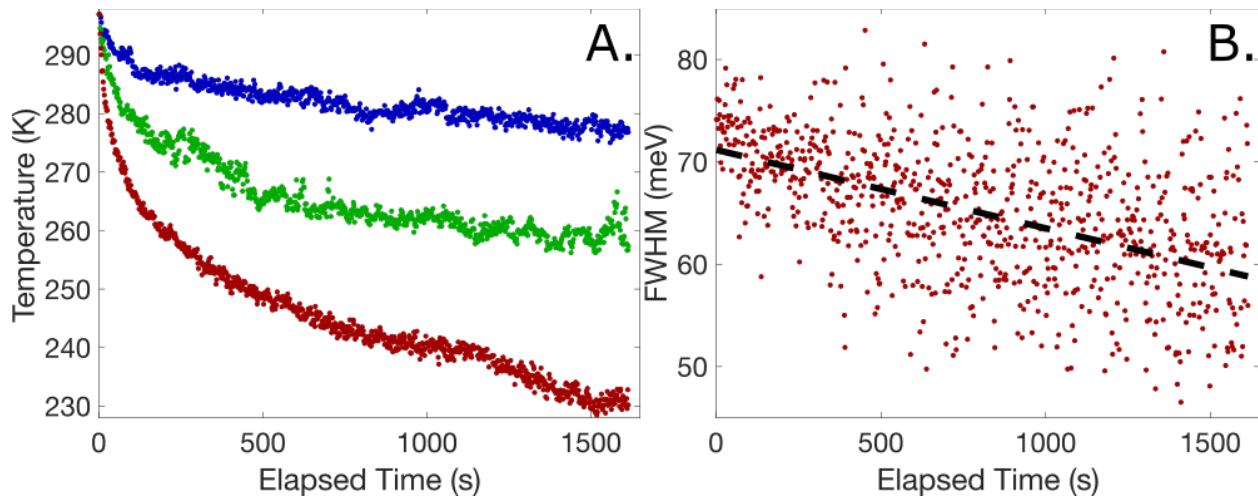


**Figure 2.** Optical cooling of CsPbBr<sub>3</sub> nanoparticles under 532 nm laser excitation. (A) CsPbBr<sub>3</sub> cooled with 532 nm excitation at a fluence of 300 (blue), 1500 (green), and 4600 (red) W/cm<sup>2</sup>. (B) ASPL full-width at half-max over time of CsPbBr<sub>3</sub> nanoparticles cooled with 532 nm excitation at a fluence of 4600 W/cm<sup>2</sup>. The dashed line is a linear fit of the data, to draw the eye.

In order to demonstrate optical cooling of CsPbBr<sub>3</sub> nanoparticles *via* ASPL, the nanoparticles were mixed into a 5% solution of polystyrene in toluene, drop-cast on a quartz slide, and placed under vacuum. Both the polystyrene encapsulation and the vacuum were used in order to thermally isolate the nanoparticles, reducing their thermal load and maximizing the observed cooling. The sample was then excited using 532 nm CW laser excitation, the resultant ASPL was collected, and equation 1 was used to determine the temperature of the nanoparticles. Figure 2 summarizes the results of this experiment.

Each absorbed and emitted photon can be thought of as a single cooling cycle. The cooling rate and the saturation temperature are dependent on the number of cooling cycles that occur per unit time. This is demonstrated in Figure 2a, where the cooling over ~25 minutes is shown for three different laser fluences: 300, 1500, and 4600 W/cm<sup>2</sup>. As expected, higher laser fluences lead to a faster cooling rate. Remarkably, at 4600 W/cm<sup>2</sup> the sample reached a temperature of 232 K, a  $\Delta T$  of  $-66$  K. This represents a new record in semiconductor cooling, as compared with the 58 K of cooling previously reported by Xiong and co-workers for 200 nm thick single crystal CH<sub>3</sub>NH<sub>3</sub>PbI<sub>3</sub> grown by chemical vapor deposition.<sup>14</sup> Additional verification that this decrease in ASPL corresponds to a decrease in temperature can be seen in the full-width at half-max (fwhm) of the ASPL (Figure 2b). A decrease in the fwhm of ASPL over the course of the measurement is consistent with a decrease in the thermal activation of carriers participating in optical recombination across the band gap. Similarly, a red-shift of the ASPL during pumping is reported in Figure S1, also indicating thermal de-activation of the energy distribution of carriers recombining across the band gap as temperature is decreased.<sup>22,23</sup>

The laser fluence not only impacts the rate of cooling, it also determines the saturation temperature—the temperature at which the thermal energy emitted by ASPL is balanced by the thermal energy gained from the local environment. This is demonstrated in Figure 3. In this experiment, the nanoparticles were excited with a 532 nm CW laser at 4600 W/cm<sup>2</sup> for ~25 minutes, during which time they cooled to a temperature of 269 K for a  $\Delta T$  of  $-28$  K. After the sample reached its saturation temperature, the laser fluence was decreased to 2300 W/cm<sup>2</sup>, half

of its original value. This decreases the rate of cooling, so that thermal energy transferred from the local environment is now greater than the thermal energy emitted through ASPL, and the sample warms up to a new saturation temperature of 280 K. Compared to room temperature, this is a  $\Delta T$  of -15 K, approximately half of the  $\Delta T$  observed for 4600 W/cm<sup>2</sup>. Intuitively, halving the fluence halves the thermal energy emitted per unit time. Increasing the laser fluence can similarly be shown to increase the rate of cooling and lower the saturation temperature (Figure S2).

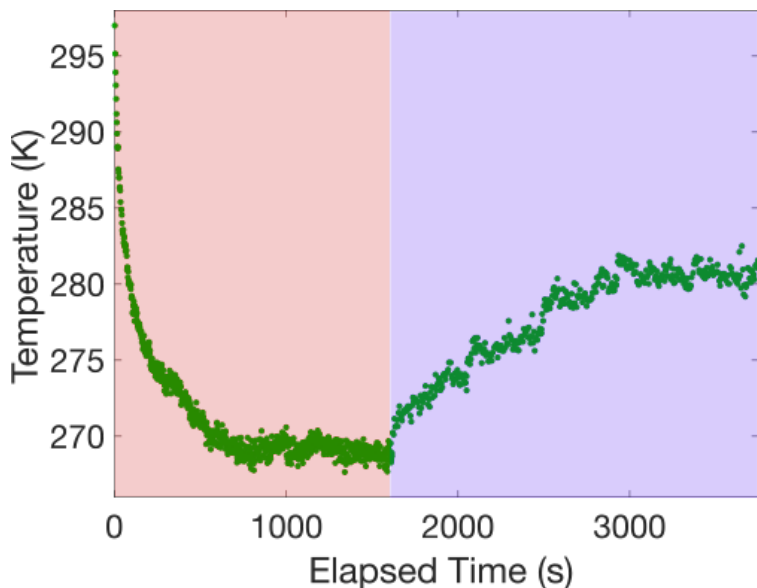


**Figure 3.** CsPbBr<sub>3</sub> cooled with 532 nm laser excitation at a fluence of 4600 W/cm<sup>2</sup> (red) followed by a laser fluence of 2300 W/cm<sup>2</sup> (blue).

The reversibility of the change in ASPL intensity is an important characteristic that differentiates the cooling observed here from photodegradation that has been observed when CsPbBr<sub>3</sub> nanoparticles are exposed to trace water, O<sub>2</sub>, or other environmental factors that degrade their electronic structure<sup>24</sup>. The reversible decrease of ASPL reported here is entirely due to a temperature change. Thus, when the excitation fluence decreases, or when the excitation pump is blocked all together (Figure S3), the ASPL intensity recovers over time as the sample warms back up. Additionally, the exponential decrease in ASPL with temperature is in direct contrast to a linear rate of PL decrease due to photodegradation. A linear decrease in PL due to photodamage can be seen in Figure S4 for a control sample of CsPbBr<sub>3</sub>. This sample was not treated with NH<sub>4</sub>SCN, and thus had PLQY less than 80%, well below the threshold required for cooling, and the nanoparticle surface was not protected by polystyrene. Rather than an exponential decrease in ASPL followed by a saturation point, the sample showed an irreversible, linear decrease over time. The ASPL fwhm also showed no significant change over time. By contrast, these results stand as further confirmation that the observed ASPL decrease in the NH<sub>4</sub>SCN-treated CsPbBr<sub>3</sub> is due to optical cooling.

In conclusion, we used the temperature dependent yield of ASPL to demonstrate optical cooling of CsPbBr<sub>3</sub> nanoparticles by upwards of 66 degrees. A remarkable aspect of these experiments is the reproducibility and consistency with which CsPbBr<sub>3</sub> nanoparticles can be optically cooled. While the rate and magnitude of the cooling are dependent on the local environment and thermal insulation of each spot analyzed in our experiments, every measurement showed an exponential

and reversible decrease in nanoparticle temperature. It is currently unclear whether the ease with which CsPbBr<sub>3</sub> nanoparticles exhibit optical cooling is a result of their unique photophysical characteristics, or whether cooling should be expected as a general feature of ASPL with near-unity EQE. Certainly, the observed cooling is comparable to that reported by Xiong and co-workers.<sup>14,15</sup> The comparison between studies suggests that the optical cooling may, in fact, be a feature of the high EQ, and the optical extraction efficiency afforded by the sub-wavelength geometry. As such, colloidal semiconductor nanoparticles with high quantum yield may likely provide an ideal platform for the study and application of optical cooling moving forward.

## References and Notes:

- (1) Sheik-Bahae, M.; Epstein, R. I. Can Laser Light Cool Semiconductors? *Phys. Rev. Lett.* **2004**, *92* (24), 247403. <https://doi.org/10.1103/PhysRevLett.92.247403>.
- (2) Roman, B. J.; Sheldon, M. The Role of Mid-Gap States in All-Inorganic CsPbBr<sub>3</sub> Nanoparticle One Photon up-Conversion. *Chem. Commun.* **2018**, *54* (50), 6851–6854. <https://doi.org/10.1039/C8CC02430H>.
- (3) Morozov, Y. V.; Zhang, S.; Brennan, M. C.; Janko, B.; Kuno, M. Photoluminescence Up-Conversion in CsPbBr<sub>3</sub> Nanocrystals. *ACS Energy Lett.* **2017**, *2* (10), 2514–2515. <https://doi.org/10.1021/acseenergylett.7b00902>.
- (4) Rakovich, Y. P.; Donegan, J. F.; Vasilevskiy, M. I.; Rogach, A. L. Anti-Stokes Cooling in Semiconductor Nanocrystal Quantum Dots: A Feasibility Study. *Phys. Status Solidi (a)* **2009**, *206* (11), 2497–2509. <https://doi.org/10.1002/pssa.200925052>.
- (5) Ye, S.; Zhao, M.; Yu, M.; Zhu, M.; Yan, W.; Song, J.; Qu, J. Mechanistic Investigation of Upconversion Photoluminescence in All-Inorganic Perovskite CsPbBr<sub>3</sub> Nanocrystals. *J. Phys. Chem. C* **2018**, *122* (5), 3152–3156. <https://doi.org/10.1021/acs.jpcc.7b12175>.
- (6) Morozov, Y. V.; Draguta, S.; Zhang, S.; Cadranet, A.; Wang, Y.; Janko, B.; Kuno, M. Defect-Mediated CdS Nanobelt Photoluminescence Up-Conversion. *J. Phys. Chem. C* **2017**, *121* (30), 16607–16616. <https://doi.org/10.1021/acs.jpcc.7b05095>.
- (7) Pringsheim, P. Zwei Bemerkungen Über Den Unterschied von Lumineszenz- Und Temperaturstrahlung. *Zeitschrift für Physik* **1929**, *57* (11–12), 739–746.
- (8) Seletskiy, D. V.; Epstein, R.; Sheik-Bahae, M. Laser Cooling in Solids: Advances and Prospects. *Rep. Prog. Phys.* **2016**, *79* (9), 096401. <https://doi.org/10.1088/0034-4885/79/9/096401>.
- (9) Frey, R.; Micheron, F.; Pocholle, J. P. Comparison of Peltier and Anti-Stokes Optical Coolings. *Journal of Applied Physics* **2000**, *87* (9), 4489–4498. <https://doi.org/10.1063/1.373614>.
- (10) Rupper, G.; Kwong, N. H.; Binder, R. Theory of Semiconductor Laser Cooling at Low Temperatures. *phys. stat. sol. (c)* **2006**, *3* (7), 2489–2493. <https://doi.org/10.1002/pssc.200668090>.
- (11) Bender, D. A.; Cederberg, J. G.; Wang, C.; Sheik-Bahae, M. Development of High Quantum Efficiency GaAs/GaInP Double Heterostructures for Laser Cooling. *Appl. Phys. Lett.* **2013**, *102* (25), 252102. <https://doi.org/10.1063/1.4811759>.
- (12) Wang, C.; Li, C.-Y.; Hasselbeck, M. P.; Imangholi, B.; Sheik-Bahae, M. Precision, All-Optical Measurement of External Quantum Efficiency in Semiconductors. *Journal of Applied Physics* **2011**, *109* (9), 093108. <https://doi.org/10.1063/1.3580259>.

- (13) Schnitzer, I.; Yablonovitch, E.; Caneau, C.; Gmitter, T. J. Ultrahigh Spontaneous Emission Quantum Efficiency, 99.7% Internally and 72% Externally, from AlGaAs/GaAs/AlGaAs Double Heterostructures. 4.
- (14) Ha, S.-T.; Shen, C.; Zhang, J.; Xiong, Q. Laser Cooling of Organic–Inorganic Lead Halide Perovskites. *Nature Photon* **2016**, *10* (2), 115–121. <https://doi.org/10.1038/nphoton.2015.243>.
- (15) Zhang, J.; Li, D.; Chen, R.; Xiong, Q. Laser Cooling of a Semiconductor by 40 Kelvin. *Nature* **2013**, *493* (7433), 504–508. <https://doi.org/10.1038/nature11721>.
- (16) Hanifi, D. A.; Bronstein, N. D.; Koscher, B. A.; Nett, Z.; Swabeck, J. K.; Takano, K.; Schwartzberg, A. M.; Maserati, L.; Vandewal, K.; van de Burgt, Y.; et al. Redefining Near-Unity Luminescence in Quantum Dots with Photothermal Threshold Quantum Yield. *Science* **2019**, *363* (6432), 1199–1202. <https://doi.org/10.1126/science.aat3803>.
- (17) Roman, B. J.; Sheldon, M. T. Six-Fold Plasmonic Enhancement of Thermal Scavenging via CsPbBr<sub>3</sub> Anti-Stokes Photoluminescence. *Nanophotonics* **2019**, *8* (4), 599–605. <https://doi.org/10.1515/nanoph-2018-0196>.
- (18) Ma, X.; Pan, F.; Li, H.; Shen, P.; Ma, C.; Zhang, L.; Niu, H.; Zhu, Y.; Xu, S.; Ye, H. Mechanism of Single-Photon Upconversion Photoluminescence in All-Inorganic Perovskite Nanocrystals: The Role of Self-Trapped Excitons. *J. Phys. Chem. Lett.* **2019**, *10* (20), 5989–5996. <https://doi.org/10.1021/acs.jpcclett.9b02289>.
- (19) Protesescu, L.; Yakunin, S.; Bodnarchuk, M. I.; Krieg, F.; Caputo, R.; Hendon, C. H.; Yang, R. X.; Walsh, A.; Kovalenko, M. V. Nanocrystals of Cesium Lead Halide Perovskites (CsPbX<sub>3</sub>, X = Cl, Br, and I): Novel Optoelectronic Materials Showing Bright Emission with Wide Color Gamut. *Nano Lett.* **2015**, *15* (6), 3692–3696. <https://doi.org/10.1021/nl5048779>.
- (20) Koscher, B. A.; Swabeck, J. K.; Bronstein, N. D.; Alivisatos, A. P. Essentially Trap-Free CsPbBr<sub>3</sub> Colloidal Nanocrystals by Postsynthetic Thiocyanate Surface Treatment. *J. Am. Chem. Soc.* **2017**, *139* (19), 6566–6569. <https://doi.org/10.1021/jacs.7b02817>.
- (21) Koscher, B. A.; Nett, Z.; Alivisatos, A. P. The Underlying Chemical Mechanism of Selective Chemical Etching in CsPbBr<sub>3</sub> Nanocrystals for Reliably Accessing Near-Unity Emitters. *ACS Nano* **2019**, *13* (10), 11825–11833. <https://doi.org/10.1021/acsnano.9b05782>.
- (22) Herrmann, F.; Würfel, P. Light with Nonzero Chemical Potential. *American Journal of Physics* **2005**, *73* (8), 717–721. <https://doi.org/10.1119/1.1904623>.
- (23) Bhattacharya, R.; Pal, B.; Bansal, B. On Conversion of Luminescence into Absorption and the van Roosbroeck-Shockley Relation. *Appl. Phys. Lett.* **2012**, *100* (22), 222103. <https://doi.org/10.1063/1.4721495>.
- (24) Rainò, G.; Landuyt, A.; Krieg, F.; Bernasconi, C.; Ochsenbein, S. T.; Dirin, D. N.; Bodnarchuk, M. I.; Kovalenko, M. V. Underestimated Effect of a Polymer Matrix on the Light Emission of Single CsPbBr<sub>3</sub> Nanocrystals. *Nano Lett.* **2019**, *19* (6), 3648–3653. <https://doi.org/10.1021/acs.nanolett.9b00689>.

**Acknowledgments:** The authors would like to acknowledge Je-Ruei Wen, Noel Mireles Villegas, Freddy Rodriguez Ortiz, and Kylie Lytle for many helpful discussions.

**Funding:** This work is funded by the Gordon and Betty Moore Foundation through Grant GBMF6882. M.S. also acknowledges support from the Welch Foundation (A-1886) and the Air

Force Office of Scientific Research under award number FA9550-16-1-0154. **Author contributions:** BJR ran the experiments, analyzed the data, and wrote the manuscript with help and input from MTS. MTS lead the project. **Competing interests:** Authors declare no competing interests. **Data and materials availability:** All data is available in the main text or the supplementary materials.

**Supplementary Materials:**

Materials and Methods

Figures S1-S4



Supplementary Materials for  
Optically Cooling CsPbBr<sub>3</sub> Nanoparticles

Benjamin J. Roman, Matthew T. Sheldon

Correspondence to: [sheldonm@tamu.edu](mailto:sheldonm@tamu.edu)

**This PDF file includes:**

Materials and Methods  
Figures S1 to S4

## Materials and Methods

### Materials

Cesium carbonate ( $\text{Cs}_2\text{CO}_3$ , Alfa Aesar, 99.995% trace metals basis), lead (II) bromide ( $\text{PbBr}_2$ , Alfa Aesar, 98+%), oleylamine (OAm, Sigma Aldrich, technical grade 70%), oleic acid (OA, Sigma Aldrich, technical grade 90%), 1-octadecene (ODE, Sigma Aldrich, technical grade 90%), hexanes (Sigma Aldrich, anhydrous mixture of isomers, 99%), toluene (Sigma Aldrich, anhydrous, 99.8%), Ammonium thiocyanate (Sigma Aldrich, 99.99% trace metals basis), polystyrene (PS, Aldrich Chemistry, average  $M_w \sim 350,000$ ).

### Preparation of Cs-oleate

$\text{Cs}_2\text{CO}_3$  (0.200 g), OA (0.624 mL), and ODE (10 mL) were added to a 25-mL 3-neck round bottomed flask and heated for 1 hour at  $120^\circ\text{C}$  under vacuum to dry. After 1 hour, the flask was put under argon and heated to  $150^\circ\text{C}$  until all the  $\text{Cs}_2\text{CO}_3$  had reacted.

### Synthesis of $\text{CsPbBr}_3$ Nanocrystals

$\text{PbBr}_2$  (0.069 g) and ODE (5 mL) were added to a 25-mL 3-neck round bottomed flask and heated under vacuum to  $120^\circ\text{C}$  for 1 hour. The solution was then placed under argon, and dried OAm (0.5 mL) and dried OA (0.5 mL) were injected to solubilize the  $\text{PbBr}_2$ . The temperature increased to  $180^\circ\text{C}$ , and the Cs-oleate (0.4 mL) was swiftly injected. After 1 minute, the solution was cooled with an ice bath. The final solution was centrifuged at 3000 g-forces for 5 minutes and the supernatant was discarded. The precipitate was dispersed in hexane.

### $\text{NH}_4\text{SCN}$ Treatment of $\text{CsPbBr}_3$ Nanocrystals

$\text{NH}_4\text{SCN}$  was added to a vial of  $\text{CsPbBr}_3$  suspended in hexane and vigorously stirred for between 20 and 30 minutes. The resulting cloudy solution was centrifuged at 3000 g-forces for 5 minutes, and the supernatant was decanted and analyzed.

### Absorbance

UV-VIS spectra from 300 to 800 nm were collected on an Ocean Optics Flame-S-UV-Vis spectrometer with an Ocean Optics DH-200-Bal deuterium and halogen lamp light source.

### Below-gap excitation photoluminescence (ASPL)

ASPL was measured using a 532 nm Nd:YAG CW laser ported through a WITec alpha 300 RA confocal microscope, focused on the sample using a long working distance 0.55 numerical aperture objective. 5  $\mu\text{L}$  of  $\text{NH}_4\text{SCN}$  treated  $\text{CsPbBr}_3$  was added to 1 mL of a 5% by w.t. solution of PS in toluene. One drop was placed on a quartz slide and allowed to dry. The sample was then placed in a Linkam Instruments TS1500 thermal stage attached to the WITec alpha 300 RA confocal microscope. Measurements were taken at a vacuum pressure  $\sim 0.010$  mBar.

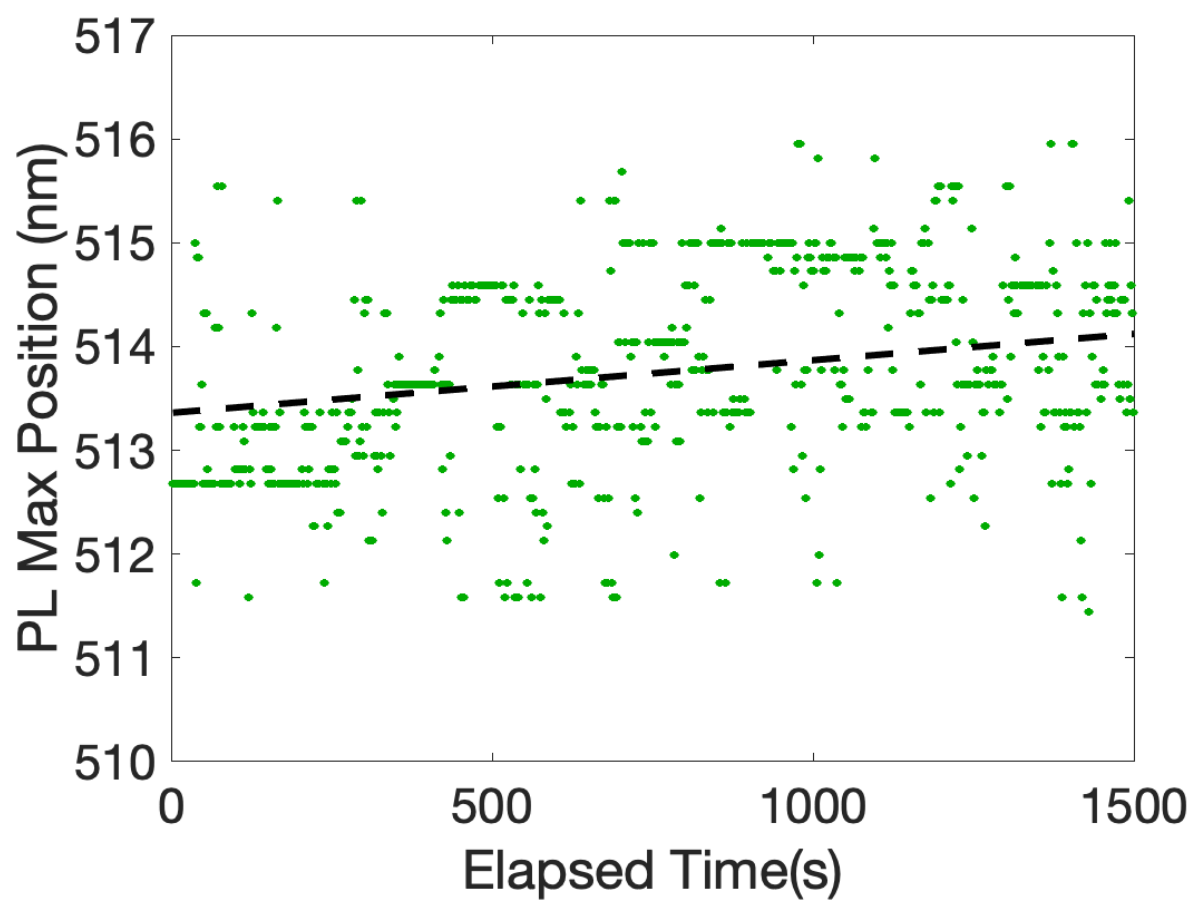


**Figure S1.**

Wavelength of ASPL maximum for CsPbBr<sub>3</sub> cooled with 532 nm excitation at a fluence of 4600 W/cm<sup>2</sup>. Dotted line is the linear fit of the data, to draw the eye.

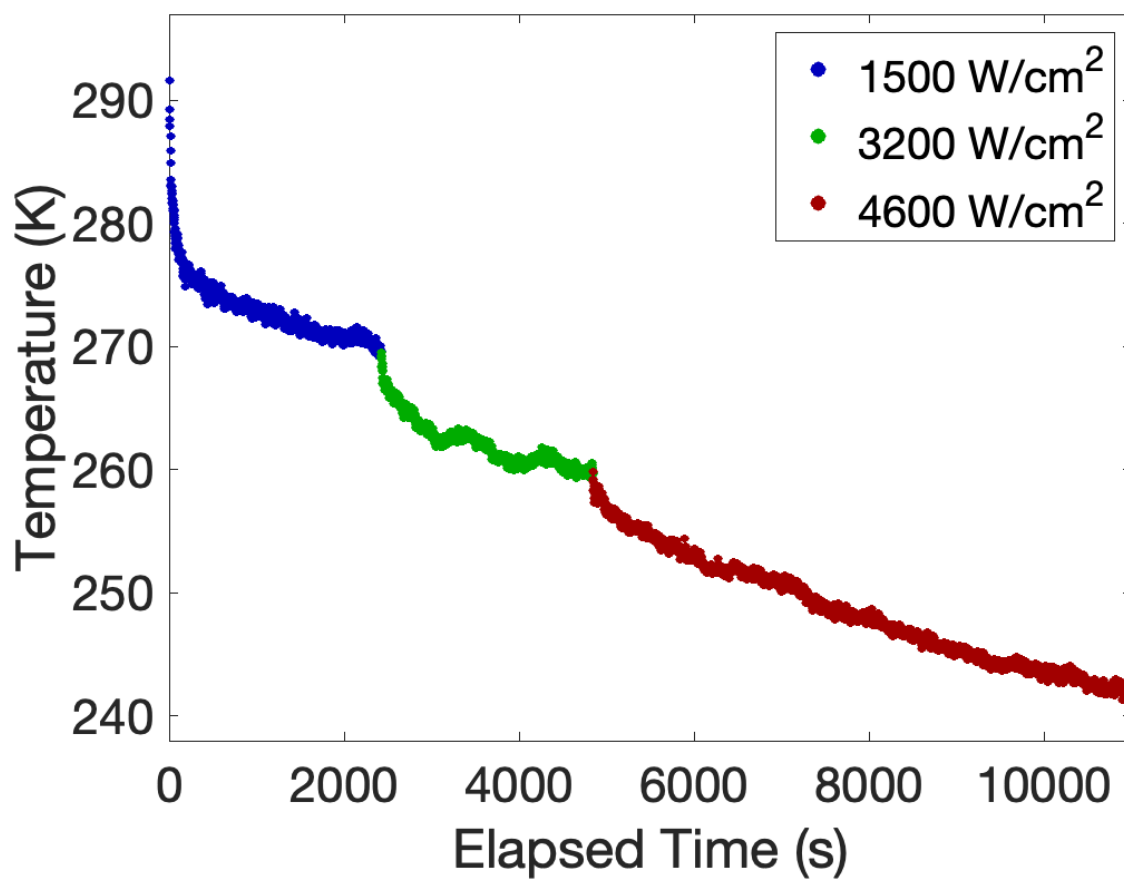


**Figure S2.**

CsPbBr<sub>3</sub> cooled with 532 nm excitation at a fluence of 1500 W/cm<sup>2</sup> (blue) followed by a laser fluence of 3200 W/cm<sup>2</sup> (green), and then 4600 W/cm<sup>2</sup> (red).

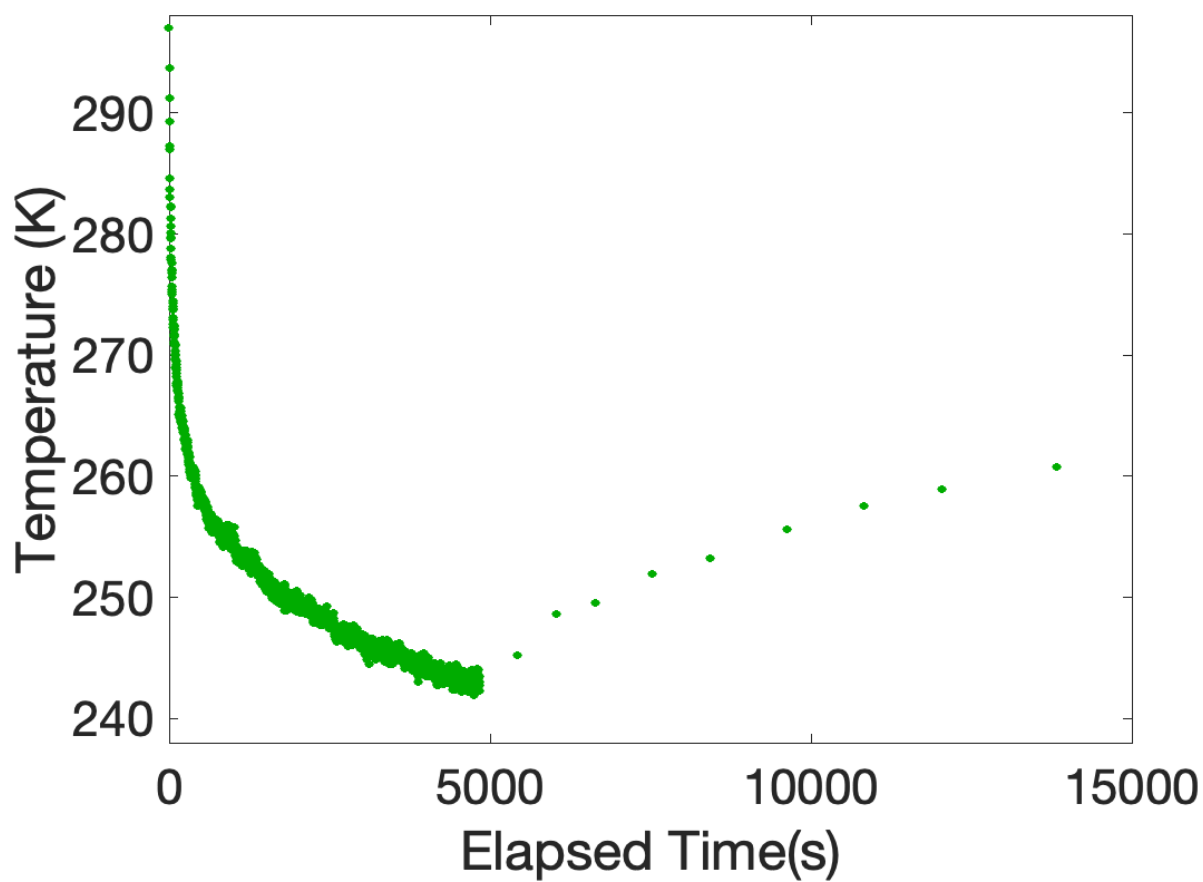


**Figure S3.**

CsPbBr<sub>3</sub> nanoparticles cooled with 532 nm excitation at a fluence of 4600 W/cm<sup>2</sup> for 5000 seconds. The laser was then blocked for a period of time to allow the sample to warm, unblocked long enough to take a spectrum, and then blocked again.

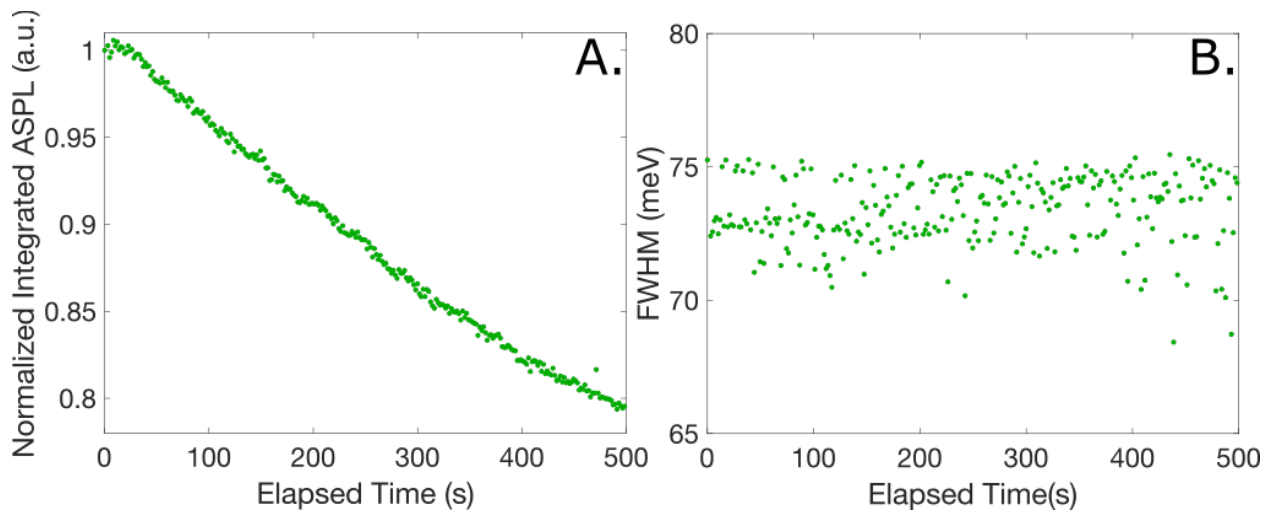


**Figure S4.**

CsPbBr<sub>3</sub> without NH<sub>4</sub>SCN treatment or PS, in open air. Excited with 532 nm excitation at a fluence of 4600 W/cm<sup>2</sup>. (A) Normalized integrated ASPL intensity over time. (B) Full-width at half-max of the sample, showing no change over time.